Theory based investigation of Outer Mode to ELM transition in JET-C plasmas

D. Brunetti[1], J. P. Graves[2], E. Lazzaro[1], A. Mariani[1], S. Nowak[1], W. A. Cooper[2], C. Wahlberg[3], E. R. Solano[4], S. Saarelma[5] and JET Contributors*

[1]*Istituto per la Scienza e Tecnologia dei Plasmi CNR, Via R. Cozzi 53, 20125 Milan, Italy*

[2]*École Polytechnique Fédérale de Lausanne (EPFL), Swiss Plasma Center (SPC), CH-1015 Lausanne, Switzerland*

[3]*Department of Physics and Astronomy, P.O. Box 516, Uppsala University, SE-751 20 Uppsala, Sweden*

[4]*Laboratorio Nacional de Fusión, CIEMAT, Madrid, Spain*

[5]*Culham Centre for Fusion Energy (CCFE), Culham Science Centre, Abingdon, UK*

Tokamak high-confinement regimes are normally affected by the presence of often violent edge localised modes (ELMs). ELMs deposit unacceptable peak heat loads causing a severe deterioration of the plasma facing components. Although several ELM control/suppression techniques have been developed, they may not be applicable to future reactors such as ITER and DEMO. Thus a vivid interest has arisen on the development of naturally ELM-free regimes. One of the most promising of such regimes is the so called quiescent high-confinement (QH) mode. In QH plasmas, ELM activity is replaced by dominantly low-n steady mild rotating MHD edge harmonic oscillations (EHOs) localised in the pedestal region. EHOs have been observed in DIII-D, ASDEX-U, JET and JT60 [1]. In JET such a MHD activity is referred to as Outer Modes (OMs) [2]. EHOs are beneficial since they enhance particle transport allowing density control and potentially ash removal without the impulsive heat load problem. Extensive numerical modelling and dedicated experiments on the DIII-D machine identify the $E\times B$ shearing rate as the key parameter which determines the accessibility of QH regimes with EHOs.

EHOs are usually observed over a fairly broad range in q_{95} ($3<q_{95}<6$) at low edge collisionality ($\nu_e^* < 0.3$) [3], with a significant bootstrap contribution to the current due to sharp edge pressure

*See the author list of "Overview of the JET preparation for Deuterium-Tritium Operation" by E. Joffrin et al. to be published in Nuclear Fusion Special issue: overview and summary reports from the 27th Fusion Energy Conference (Ahmedabad, India, 22-27 October 2018)

gradients. Within the framework of the ideal drift-MHD model [4,5] we are able to identify the specific physical mechanism governing the onset of these instabilities. They have features of both external kink modes (distorted plasma boundary with a vacuum region between plasma and wall needed to achieve good detachment) and infernal modes (mode coupling driven by large pressure gradients and low local magnetic shear). We call these modes *exfernal modes* [5]. Due to the combined effect of toroidicity and flows (both MHD and diamagnetic in the toroidal and poloidal directions), short wavelength modes ($m \gg 1$) are entirely suppressed, while low- n (i.e. moderately low- m) are allowed to grow as shown by the dispersion relation [5]:

$$\frac{\gamma}{\omega_A} \approx n\sqrt{\frac{\Lambda(\beta q)^2}{4\mathfrak{D}\varepsilon^2} - \frac{\delta q^2}{q^4} - \left(\frac{m^2 q \omega_E \Delta}{2\mathfrak{D}\omega_A}\right)^2}, \qquad \frac{\omega}{\omega_A} \approx n\Omega, \tag{1}$$

where γ is the growth rate and ω the mode rotation frequency, ω_A the Alfvén frequency, $\beta = p_{ped}/B_0^2$, Λ accounts for mode coupling and $\mathfrak{D} \sim m$ for $m \gg 1$ (a detailed expression of these two quantities can be found in [5]), ε is the inverse aspect ratio, ω_E and Ω are the $E\times B$ and pedestal toroidal rotation frequencies respectively while Δ indicates the pedestal width and q is the safety factor value in the edge low shear region. The dispersion relation above shows that these instabilities are driven by the weakness of the magnetic shear and by a sufficiently large β value at the pedestal top. The strength of the $E\times B$ rotation frequency determines the suppression of the short wavelength modes. In order to have large β, either temperature or density (or both) can be increased. We note however that a density increase (for a given T_e) is associated with an increase of collisionality and subsequently a loss of bootstrap contribution to the current might be expected [6]. This in turn affects the safety factor profile by increasing the local (pedestal) magnetic shear. Therefore, the dispersion relation (1), suggests that *exfernal* modes are more likely to occur in regimes which have a moderately small density and high temperatures at the pedestal. It is worth pointing out that the *exfernal* model [5] reproduces several experimental features such as mode rotation frequencies, radial structure, amplitude of the critical $E\times B$ shearing rate. The next step is to apply the findings represented by (1) to JET experimental data interpretation.

We identified three JET-C pulses (#74511, 78012, 79455 which are the most interesting representatives out of 10 shots with similar behaviour), having comparable values of plasma current, toroidal magnetic field, edge safety factor and Z_{eff} ($I_p \approx 2.5\ MA,\ B_0 \approx 2.5\ T, q_{95} \approx 3.3$,

$Z_{eff} \approx 2$). The NBI injected power is $\approx 15, 17, 11\ MW$ for discharges #74511, 78012, 79455 respectively. They all exhibit pedestal localised OM activity (MHD of nature) clearly visible on Mirnov and ECE signals, with the fundamental ($n = 1$) harmonic rotating at $\sim 6\ kHz$. The mode appears at the initial phase of the discharge directly after the switching on of the NBI, and its lifetime is of the order of 1 s (ranging from 0.6 s to 1 s depending on the discharge). The mode onset is characterised by rather large pedestal temperatures ($T_i \sim 2\ keV$ from CSXE, $T_e \sim 1.5\ keV$ from HRTS) and moderately low densities ($n \sim 4{\times}10^{19}\ m^{-3}$ from HRTS) with the toroidal carbon velocity of the order of $100 - 150\ km/s$ (from CSXE). The mode appearance is associated with the temperature rise due to the NBI, indicating a β dependent drive. A steady density increase accompanies the mode lifetime, until the quiescent OM phase is lost and the discharge enters a high density regime with ELMs (this is shown in fig. 1). Since there is no substantial change in the edge total pressure value (i.e. the α ballooning parameter) from the QH to the ELM phase (see figure 2-a), we can rule out variations in the pressure gradient as responsible for the OM disappearance. It can be seen in figure 2-b that, although having an almost constant NBI, the rotation amplitude at the pedestal top significantly decreases its value after entering the ELMing regime. In Ref. [2] a connection between toroidal (carbon) rotation shear and OM phase was established, however numerical simulations and experimental DIII-D findings [7,8] showed a weak dependence of the accessibility of the QH phase upon the strength of the gradient of the toroidal (carbon) rotation. Hence, in this work we focus our attention on the consequences following the increase of the pedestal density value. It is found that the electron

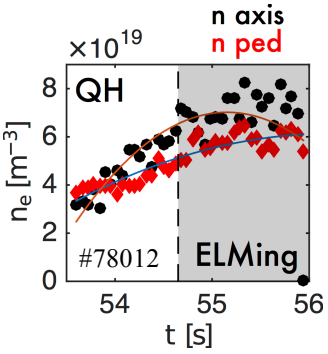

Figure 1: Density evolution (core in black, pedestal top in red) for the discharge #78012. The QH to ELMing trasition is highlighted.

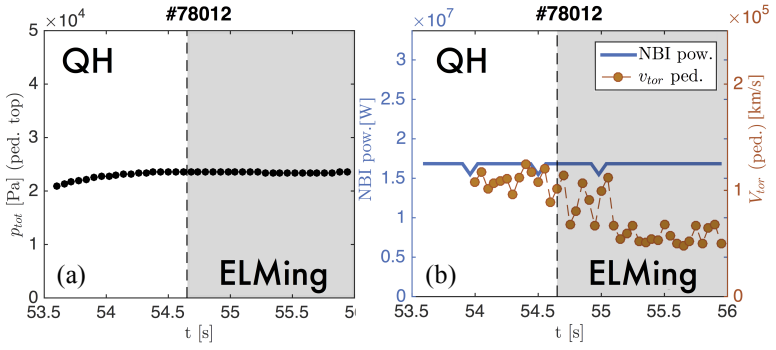

Figure 2: (a) Total pressure behaviour and (b) NBI power and carbon toroidal rotation at the pedestal top vs time for JET discharge #78012. The dashed vertical line indicates the appearance of the first ELM after which the QH phase is not recovered anymore. A significant variation of the toroidal rotation is observed in the ELM phase.

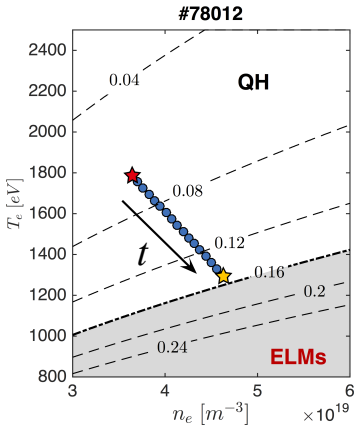

Figure 3: Time evolution (indicated by the arrow) of the (n_e, T_e) state of discharge #78012 from t=53.6s (red star) until t=54.65s (yellow star). The dashed lines indicate ν_e^* levels [9]. Once the $\nu_e^* \sim 0.16$ is crossed (thick dot-dashed line) the OM is lost and ELMs appear.

temperature decreases, while maintaining $\alpha \sim const$ (cf. fig 2-a). These two effects combined produce an increase of the edge electron collisionality. Once the pedestal density reaches a threshold value (falling for the three discharges in the range of $5-6\times10^{19}m^{-3}$) the OM is lost and ELMs appear (cf. Figs. 1 and 3). Hence, we have the logical sequence:

$$n \nearrow, T_e \searrow (\alpha \sim const) \Longrightarrow \nu_e^* \nearrow \Longrightarrow J_{bs} \searrow \Longrightarrow \hat{s} \nearrow,$$

where J_{bs} is the boostrap current and $\hat{s}$ is the magnetic shear in the pedestal region. We modify the dispersion relation (1) by substituting the term $-\delta q^2/q^4$ with $-(\hat{s}\Delta/q)^2$ (associated with the loss of weak magnetic shear). Thus, as the magnetic shear increases (due to the loss of bootstrap current) the *exfernal* drive becomes weaker (eventually stabilised for sufficiently large $\hat{s}$). Hence, the ballooning second region of stability boundary can be crossed, potentially implying the appearance of ELMs associated with these modes and consequently the loss of the QH phase. Work is currently ongoing in order to assess whether OM activity in JET could be identified with metallic (W) wall conditions. Although the pedestal temperature is higher, in general, with a carbon wall, as long as a sufficiently large β and small ν_e^* are maintained at the pedestal, *exfernal* instability (viz. EHOs/OMs) can be possible with a W wall as shown by recent studies on ASDEX-U [10].

References:

[1] E. Viezzer *et al.*, Nucl. Fusion **58**, 115002 (2018)

[2] E. R. Solano *et al.*, Phys. Rev. Lett. **104**, 185003 (2010)

[3] X. Chen *et al.*, Nucl. Fusion **56**, 076011 (2016)

[4] D. Brunetti *et al.*, Nucl. Fusion **58**, 014002 (2018)

[5] D. Brunetti *et al.*, Phys. Rev. Lett. **122**, 155003 (2019)

[6] S. Saarelma *et al.,* Nucl. Fusion **53** 123012 (2013)

[7] F. Liu *et al.*, Plasma Phys. Control. Fusion **60**, 014039 (2018)

[8] A. M. Garofalo *et al.*, Nucl. Fusion **51**, 083018 (2011)

[9] O. Sauter *et al.*, Phys. Plasmas **6**, 2834 (1999)

[10] H. Meyer *et al.*, "Overview of Physics Studies on ASDEX Upgrade", Nucl. Fusion *in press* (2019)

This work has been carried out within the framework of the EUROfusion Consortium and has received funding from the Euratom research and training programme 2014-2018 and 2019-2020 under grant agreement No 633053. The views and opinions expressed herein do not necessarily reflect those of the European Commission. This work was supported in part by the Swiss National Science Foundation.